Spin-glass behavior in the $S=1/2$ fcc ordered perovskite Sr_2CaReO_6

C. R. Wiebe, J. E. Greedan, and G. M. Luke
The Brockhouse Institute for Materials Research, McMaster University, Hamilton, Ontario, Canada L8S 4M1

J. S. Gardner
Neutron Program for Materials Research, NRC, Chalk River Labs, Chalk River, Ontario, Canada K0J 1J0
(Received 18 October 2001; published 27 March 2002)

The ordered perovskite Sr_2CaReO_6 of monoclinic symmetry [space group $P2_1/n, a=5.7556(3)$ Å, $b=5.8534(3)$ Å, $c=8.1317(4)$ Å, $\beta=90.276(5)°$ at $T=4$ K] has been synthesized using standard solid-state chemistry techniques. The difference in the size and charge of the cations induces an ordering of the *B* site Ca^{2+} and Re^{6+} ions which leads to a distorted fcc lattice of spin-$\frac{1}{2}$ Re^{6+} ($5d^1$) moments. dc magnetic susceptibility measurements indicate a maximum at $T_G \sim 14$ K and an irreversibility in the field-cooled and zero-field-cooled data at ~22 K that is believed to be caused by the geometric frustration inherent in the fcc structure. Neutron-scattering measurements confirm the absence of magnetic long-range order, and muon spin relaxation experiments indicate the presence of an abrupt spin freezing at T_G. Specific heat measurements reveal a broad anomaly typical of spin glasses and no sharp feature. 65% of the spin entropy is released at low temperatures. The low-temperature data do not show the expected linear temperature dependence, but rather a T^3 relationship, as is observed, typically, for antiferromagnetic spin waves. The material is characterized as an unconventional, essentially disorder-free, spin glass.

DOI: 10.1103/PhysRevB.65.144413 PACS number(s): 75.50.Lk, 74.25.Ha, 61.12.−q, 76.75.+i

INTRODUCTION

The topic of geometric frustration has been at the forefront of condensed-matter physics for the last decade due to the remarkable variety of interesting magnetic ground states observed.[1–3] The availability of lattice types which can accommodate the requisite triangular motif of spins coupled with the variety of magnetic species to place on these sites has led to the discovery of a number of materials which have been central to the development of this new subfield of magnetism. Some of these systems appear to order on intermediate length scales at low temperatures, such as the garnet $Gd_3Ga_5O_{12}$.[4] Others, instead, exhibit phase transitions to disordered or very short-range ordered states such as the unconventional spin glasses $SrCr_{9p}Ga_{12-9p}O_{19}$ (Ref. 5) and $Y_2Mo_2O_7$ (Ref. 6). In the last few years, the focus of study has shifted to a search for more exotic states such as the spin liquid, which arises due to quantum effects from networks of frustrated spin-$\frac{1}{2}$ moments, or the spin ice, which is related to the problem of proton disorder in hexagonal water ice first discussed by Pauling.[7] For example, the pyrochlore $Dy_2Ti_2O_7$ has been identified as a spin ice material.[8] Such discoveries provide the impetus to look for new materials.

Despite this high level of interest, the number of examples of frustrated systems with isolated spin-$\frac{1}{2}$ moments is relatively small. $LiNiO_2$, for example, is believed to have a quantum spin-liquid ground state which is stabilized by short-ranged ferromagnetic correlations,[9] but sample quality is an issue which is still being addressed. Spin-liquid characteristics have been found in other materials such as $Tb_2Ti_2O_7$, where Tb^{3+} is an effective $S=\frac{1}{2}$ ion at low temperatures.[10] Attention has turned recently to less conventional $S=\frac{1}{2}$ systems such as those based on Re^{6+} ($5d^1$). For example, Li_4MgReO_6 where the Re^{6+} sublattice consists of a three-dimensional array of face-sharing tetrahedra has been synthesized and characterized.[11] Its behavior is spin-glass-like with some unconventional features. While the Re^{6+} sublattice is disorder free, mixing of Li^+ and Mg^{2+} on adjacent sites may induce the spin-glass-like ground state. To date the number of systems with very little disorder and well-defined $S=\frac{1}{2}$ moments on frustrated lattices is still small.

The perovskites have historically proved themselves to be extremely robust structures that can accommodate a wide variety of cations on the *A* and *B* sites. For certain combinations of oxidation states and cation radii, cation ordering is well known to exist, such as in the perovskites $A_2BB'O_6$ (B^{2+}, B'^{6+}).[12] These ordered sublattices of *B* and *B′* sites form two interpenetrating fcc networks, which do indeed fall into the class of frustrated materials, since an fcc lattice is comprised of a network of edge-shared tetrahedra. The number of systems that have been investigated as candidates for geometric frustration on fcc lattices is relatively small as well. Sr_2NbFeO_6 for example, with $S=\frac{5}{2}$ $3d^5$ Fe^{3+} spins, has demonstrated spin-glass behavior according to Rodriguez *et al.*,[13] however, the *B*-site ordering is incomplete in this material. Recently, the $S=1$ systems Sr_2NiTeO_6 and Sr_2NiWO_6 have been studied by Iwanaga *et al.*, but they have been found to order at low temperatures.[14] Reports of $S=\frac{1}{2}$ materials of this class are sparse.

This paper details the synthesis and characterization of a spin-$\frac{1}{2}$ frustrated material with Re^{6+} $5d^1$ ions on an fcc lattice. The perovskite Sr_2CaReO_6 exhibits frustration effects in the absence of detectable disorder on the Re sites. This is one of the few detailed studies to our knowledge of an ordered spin-$\frac{1}{2}$ system on an edge-shared network of tetrahedra.

EXPERIMENTAL PROCEDURES

Polycrystalline samples of Sr_2CaReO_6 were prepared by firing stoichiometric quantities of SrO (99.9%, Fisher), CaO

(99.99%, Cerac), and ReO_3 (99.9%, Rhenium Alloys, Inc.) under vacuum for 60 h at 900 °C in platinum crucibles.

$$2SrO+CaO+ReO_3 \rightarrow Sr_2CaReO_6.$$

The reactants SrO and CaO were first prefired under vacuum for 12 h at 400 °C to eliminate surface impurities and remove any absorbed water. The final product was found to be multiphasic, so a subsequent regrinding and refiring stage was needed to isolate a single phase product.

The quality of the final product was analyzed using a focussing Guinier-Hägg camera with copper $K_{\alpha 1}$ radiation and a high-purity Si powder as an internal standard. No impurities were initially detected by this technique. The oxygen stoichiometry was measured using thermogravimetric analysis, by heating the sample to 900 °C under flowing hydrogen.

Neutron diffraction was also carried out on this material using the C2 diffractometer at the National Research Council's Neutron Program for Materials Research in Chalk River, Canada. Two different wavelengths were employed to investigate the possibility of magnetic ordering [2.3688(3) Å] and to obtain an accurate structural refinement [1.3284(2) Å]. The powder patterns were obtained in a temperature range of 4–40 K using a helium cryostat.

dc magnetic susceptibility data were obtained using a Quantum Design MPMS superconducting quantum interference device magnetometer at McMaster University. Field-cooled (FC) and zero-field-cooled runs (ZFC) were carried out over a temperature range of 2 to 350 K with applied magnetic fields of 0.01 and 0.1 T. Isothermal magnetization data were obtained at temperatures of 5, 25, and 40 K in applied fields to 5.5 T.

The heat capacity was measured using an Oxford Instruments Calorimeter, a probe in the Oxford Instruments MagLab system. The sample was a pellet weighing 26.75 mg, and a small known portion of Wakefield grease was applied to insure good thermal contact for which a correction was made. The measurements were completed between 4 and 35 K using the relaxation method. The sample itself was attached to a sapphire platform which has a Cernox-chip thermometer for temperature control. Measurements at both zero field and an applied field of 6 T were taken in the same temperature range for the Sr_2CaReO_6 sample.

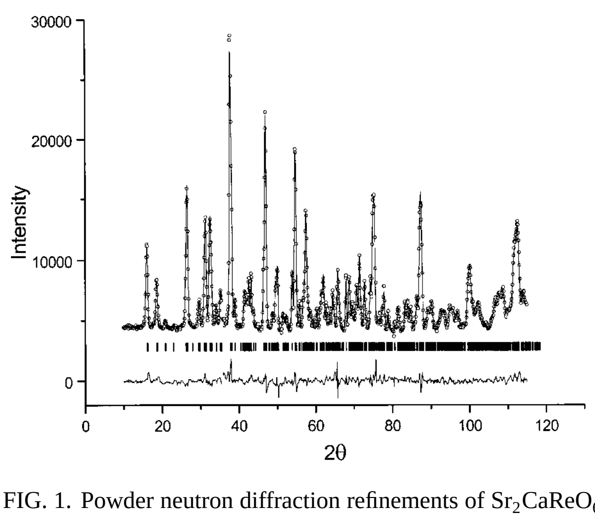

FIG. 1. Powder neutron diffraction refinements of Sr_2CaReO_6 at $T=4$ K with $\lambda=1.3284(2)$ Å neutrons ($R_p=7.87, R_{wp}=9.03$).

TABLE I. Lattice parameters for Sr_2CaReO_6 at 4 K (short wavelength neutron data) and 295 K (x-ray data) as determined by powder diffraction. The material used as a model for the lattice contribution to the heat capacity, orthorhombic Sr_2CaWO_6, is referenced as well for comparison (x-ray data).

	Sr_2CaReO_6, 4 K	Sr_2CaReO_6, 295 K	Sr_2CaWO_6, 295 K
a	5.7556(3) Å	5.7582(3) Å	5.7657(2) Å
b	5.8534(3)	5.8346(3)	5.8496(3)
c	8.1317(4)	8.1787(4)	8.1927(4)
β	90.276(5)°	90.245(3)°	90°

The muon spin relaxation (μSR) experiments were completed at TRIUMF in Vancouver, Canada. The measurements were carried out over a temperature range of 2.5–39.5 K with zero applied magnetic field.

RESULTS AND DISCUSSION

A. Crystal structure

After the initial firing, the reaction product was found by powder x-ray diffraction to consist of two phases, one monoclinic and the other cubic, by indexing the lines using the search routine DICVOL.[15] Regrinding and refiring under vacuum yielded only the monoclinic phase as the final product.

The space group was determined to be $P2_1/n$ consistent with the Ca_2SrReO_6 phase reported by Chamberland and Levasseur.[16] As noted, it is isostructural with the monoclinic Ca_3WO_6 phase. Similar structures have been reported before by Jung and Demazeau[17] for the iridium analog Sr_2CaIrO_6 and the related compounds Sr_2NiTeO_6, by Iwanaga *et al.*[12] The unit cell constants at room temperature were found to be $a=5.7582(3)$ Å, $b=5.8346(3)$ Å, $c=8.1787(4)$ Å, and

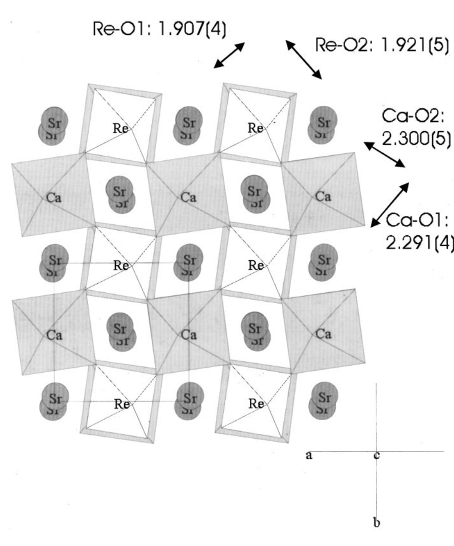

FIG. 2. The crystal structure of Sr_2CaReO_6 as viewed from the *ab* plane at $T=4$ K. Note the distortion of the Ca and Re octahedra.

TABLE II. Refined lattice positions and temperature factors for Sr_2CaReO_6 [$\lambda=1.3284(2)$ Å] at 4 K.

	x	y	z	B	Site
Sr	0.0096(8)	0.0421(4)	0.2477(8)	0.80(10)	4e
Ca	0.5	0.0	0.0	0.56(8)	2d
Re	0.5	0.0	0.5	0.54(8)	2c
O1	0.2664(8)	0.3109(8)	0.0384(7)	0.86(10)	4e
O2	0.1861(8)	−0.2342(9)	0.0468(6)	0.96(10)	4e
O3	−0.0822(7)	0.4769(7)	0.2256(5)	0.82(10)	4e

$\beta=90.245(3)$ Å using the program LSUDF.[18] There were no impurity lines found. Previously, an orthorhombic cell with similar lattice parameters ($a=5.76$ Å, $b=5.85$ Å, $c=8.21$ Å),[19] and a cubic cell with $a=8.198(5)$ Å have been reported for this material.[16] No reports of the monoclinic structure have been published to date, but it is likely that the small deviation from orthorhombic symmetry was not detected in earlier efforts. This distortion becomes more pronounced at low temperatures (Table I).

The crystal structure was refined from neutron-powder-diffraction data at 4 K using the Rietveld refinement suite FULLPROF.[20] The refinements revealed a small impurity at $d=2.14$ Å which could not be indexed. This peak was excluded in the final refinements (see Fig. 1). The final atomic positions at 4 K are listed in Table II.

The ordered perovskite structure of monoclinic Sr_2CaReO_6 is shown in Figs. 2 and 3. The distortion away from cubic symmetry is due to two factors: the presence of a relatively small cation on the A site and the mismatch of cations on the B and B' sites. A choice of Ba^{2+} for the A site, which has a significantly larger ionic radius than Sr^{2+},[21] (1.75 Å compared to 1.58 Å for XII coordinated sites) results in a readily obtained cubic structure Ba_2CaReO_6, by the same synthesis techniques.[22] The larger framework in this case provides more volume for the B sites and thus a more accommodating structure. A choice of a smaller cation than Ca^{2+} on the B site, such as Mg^{2+} which has an ionic radius more similar in size to Re^{6+}, results in a tetragonal unit cell

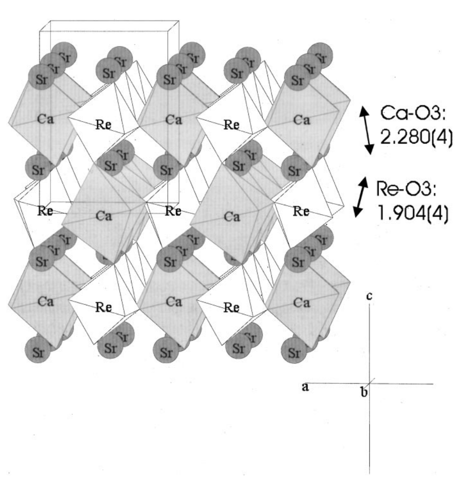

FIG. 3. The crystal structure of Sr_2CaReO_6 as viewed from the ac plane.

as in Sr_2MgReO_6 (Ca^{2+} has a radius of 1.14 Å, as compared to 0.86 and 0.69 Å for Mg^{2+} and Re^{6+} VI coordinated sites, respectively).[23] The possibility of disorder on the B sites is more likely here though, with such similar sizes of cations. The goal in the synthesis of Sr_2CaReO_6 was to find a material with an ordered array of Re^{6+} moments on an fcc lattice to study the effects of geometric frustration in the absence of disorder.

Nonetheless, the possibility for cation disorder was investigated in the refinements by allowing for site mixing among the A, B, and B' cation sites. All of the atoms refined to full occupancy on their respective sites to within 1%. Disorder in this structure is highly unlikely due not only to the differences in sizes of the cations, but also due to the large difference in formal charge on the B and B' site ions. The electrostatic repulsion between the Re^{6+} cations is a significant ordering mechanism.

The bond lengths of the Re^{6+} and Ca^{2+} octahedra are listed in Figs. 2 and 3, and noted in Table III. All of the octahedra are distorted, with unequal apical and equatorial bond lengths as indicated. A valence bond sum analysis was carried out using VALIST (Ref. 24) to determine the oxidation state of the Re ions. The elongated bonds on the Re octahedra gave slightly higher values for the valence (7+ rather than 6+), and the Ca octahedra being similarly distorted

TABLE III. Bond distances and angles for Sr_2CaReO_6 at $T=4$ and 20 K as determined by powder neutron diffraction [$\lambda=1.3284(2)$ Å]. There are no appreciable changes due to the phase transition at $T_G\sim14$ K.

	4 K	20 K
Re-O1	1.907(4) Å	1.899(5) Å
Re-O2	1.921(5)	1.925(5)
Re-O3	1.904(4)	1.908(4)
Ca-O1	2.291(4)	2.297(4)
Ca-O2	2.300(5)	2.295(5)
Ca-O3	2.280(4)	2.280(4)
Re-Re	5.7518(3)	5.7483(3)
	5.7640(2)	5.7652(2)
	5.7835(2)	5.7859(2)
	5.8494(3)	5.8468(2)
Re-O2-Ca	152.562(184)°	152.445(179)°
Re-O1-Ca	155.278(172)	155.356(168)
Re-O3-Ca	152.269(162)	152.442(156)

gave slightly higher values as well (2.5+ rather than 2+). The high values for the Re site reflect the poorly known valence bond parameters for the Re^{6+} species. To address this problem, a thermogravimetric analysis in flowing hydrogen was completed to fully reduce the sample by heating to 900 °C. The expected reaction is

$$Sr_2CaReO_6 + 3H_2 + \rightarrow 2SrO + CaO + Re + 3H_2O.$$

The experimental weight loss of 10.25% correlated quite well with the expected weight loss of 10.14% assuming full oxygen stoichiometry, and thus an oxidation state of Re^{6+}. The final product, a dull yellow colored solid, was investigated using x-ray diffraction on the Guinier-Hagg apparatus mentioned above and was found to contain Re metal and a mixture of poorly crystallized $Sr_xCa_{1-x}O$ phases. The oxygen stoichiometry was assumed to be 6.0, but in the final refinements of the neutron data, the occupancy factors for each oxygen site were allowed to vary to check for defects. The values refined to their full occupancies to within 1%.

Since the magnetic interactions between the Re moments are mediated via superexchange mechanisms, the bond angles for the Re-O-Ca-O-Re pathways are important to note at this point. Due to the significant tilting in the octahedra of the distorted structure, these angles vary greatly from the ideal 180° for the perfect cubic structure, as indicated in Table III.

The underlying topology of the magnetic sublattice, however, suggests that magnetic frustration should be observed due to the Re^{6+} ordering on the fcc lattice. Figure 4 shows the isolated Re sublattice with respect to the unit cell. The bond distances have been indicated in angstroms. Although these distances are not equal due to the low symmetry of the monoclinic framework, they all lie within a few percent of the mean distance (~5.8 Å), and the magnetic exchange constants are expected to be similar for nearest neighbors on all of the Re sites.

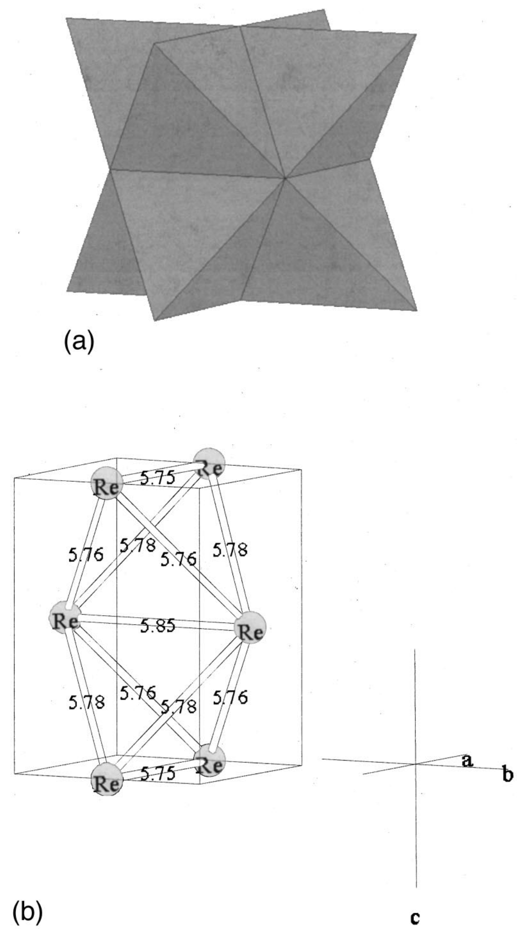

FIG. 4. The ordered Re ions in the fcc-based lattice form a network of edge-shared tetrahedra as indicated above. The corresponding Re-Re distances are noted in the figure below.

B. Magnetic susceptibility experiments

The magnetic response of Sr_2CaReO_6 was expected to be quite weak due to the dilute nature of the magnetic sublattice and relatively small size of the Re^{6+} moment. Previous dc susceptibility measurements on the ordered perovskite Sr_2CaReO_6 in the range of 80–300 K suggested Curie-Weiss behavior, with $\theta = -189$ K and an effective moment of $\mu_{eff} = 1.08\mu_B$ based upon a fit to[16]

$$\chi = C/(T-\theta), \tag{1}$$

where $\mu_{eff} = \sqrt{8}$ C. The values obtained here by fitting over the temperature range of 170–250 K (see inset, Fig. 5) are $\mu_{eff} = 1.659(6)\mu_B$ and $\theta = -443(6)$ K (after applying a diamagnetic correction). This indicates strong antiferromagnetic interactions among the Re moments, a requirement for geometric frustration. The strong antiferromagnetic interactions are perhaps unexpected in this material, considering the distorted exchange pathways and small values for the Re $S = \frac{1}{2}$ moments. One possible reason for this result is due to the extended nature of the $5d$ orbitals, which provide good overlap regardless of the deviations in bond angle. One can compare this system with the monoclinic Ni analog Sr_2NiTeO_6, with a $3d^8$ configuration $S=1$ on the Ni^{2+} site, which has a Weiss constant of -240 K.[14] From mean-field theory, one can compute values for the nearest-neighbor exchange constant as

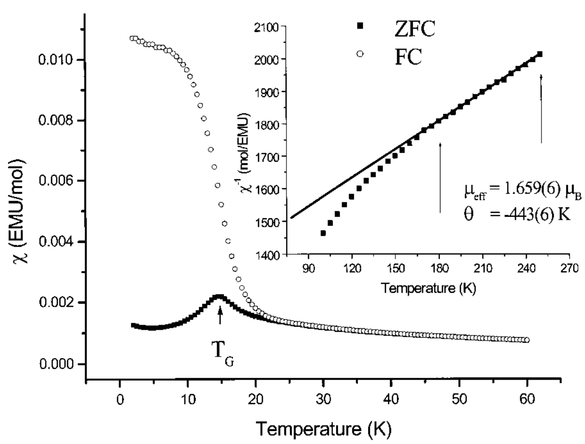

FIG. 5. dc magnetic susceptibility results for powder Sr_2CaReO_6 samples. The inset shows the inverse susceptibility, and the fit to the Curie-Weiss law as indicated in the text.

$$J_{nn}/k = \frac{\theta_c}{12(2/3)S(S+1)}. \qquad (2)$$

The ratio of J_{nn}/k for Sr_2CaReO_6 relative to Sr_2NiTeO_6 is 5:1, which illustrates the more extended nature of the $5d$ orbitals relative to $3d$ orbitals.

The value obtained for the effective moment falls slightly shy of the theoretical value for a $5d^1$ system, which is expected to be $1.73\mu_B$ for $S=\frac{1}{2}$. It is well known, however, that Re^{6+} in an octahedral environment has a reduced magnetic moment due spin-orbital coupling and crystal-field effects. These spin-orbital contributions have been noted to reduce the moment in related systems as well, such as Li_4ReMgO_6, which has an effective moment of $1.14(1)\mu_B$ on the Re^{6+} sites.[10] Reduced moments are also a signature of geometrically frustrated systems, with many known cases in the literature.[2]

Another common feature of geometrically frustrated materials is a divergence in the field-cooled and zero-field-cooled susceptibility at low temperatures, indicative of a highly degenerate magnetic ground state. The cusplike feature that is observed in Fig. 5 is seen in other frustrated materials, such as the pyrochlore spin glass $Y_2Mo_2O_7$, which has a network of corner-shared tetrahedra.[6] A major difference in the magnetic response of our sample is a divergence in the susceptibility at $T\sim 23$ K which occurs at temperatures much higher than the transition temperature of $T_G\sim 14$ K, where the cusp is located. This suggests the presence of magnetic correlations which set in at a higher temperature scale than T_G.

Additional evidence for frustration effects in this material is seen in the Curie-Weiss fit to the inverse susceptibility, which lies above the data at low temperatures, inset, Fig. 5. This departure from Curie-Weiss behavior is not well understood, but it is believed to be due to orphan spins, or spins due to defects, for systems that display structural disorder.[2] However, this feature is seen in frustrated materials with very little or no structural disorder as well, such as the spin ice $Dy_2Ti_2O_7$ (Ref. 8) or the spin glass $Y_2Mo_2O_7$.[6] Clearly, an explanation for this characteristic still lacks solid theoretical grounding, but progress is being made.[25]

Finally, a frustration index f_{frus} is typically used as a measure of the degree of frustration in a magnetic material, which is defined as

$$f_{\mathrm{frus}} = |\theta|/T_{\mathrm{ord}}, \qquad (3)$$

where θ is the Weiss temperature as extracted from the high-temperature Curie-Weiss fits, and T_{ord} is a transition temperature. Typically, for geometrically frustrated materials $f_{\mathrm{frus}}>10$. The f_{frus} for Sr_2CaReO_6 can be estimated at ~ 31. In comparison to other perovskites, Sr_2NbFeO_6 has a $f_{\mathrm{frus}} \sim 30$ and is a spin glass, but the role of B site disorder is unclear.[13] The $S=1$ ordered analogs Sr_2NiTeO_6 and Sr_2NiWO_6 have lower indices of $f_{\mathrm{frus}}\sim 7$ and $f_{\mathrm{frus}}\sim 3$, and they form ordered ground states.[14] The observation of glassy magnetic behavior is thus expected for Sr_2CaReO_6 as well.

The cusplike feature and divergence in the FC/ZFC susceptibility is a tell-tale sign of a spin-glass transition, yet

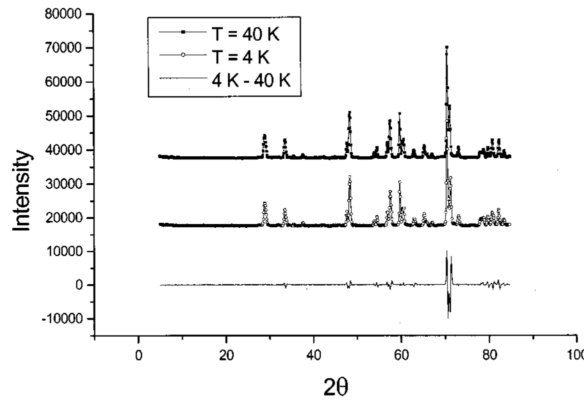

FIG. 6. Powder-neutron-diffraction profiles at $T=4$ K and $T=40$ K with $\lambda=2.3688(3)$ Å. Note the absence of magnetic Bragg peaks in the difference profile below. The shift observed is due to a slight relaxation of the lattice as the temperature is increased.

these features have also been seen in samples that exhibit long-range magnetic ordering. Even though the magnetic sublattice is highly frustrated, such an ordering is always possible, and to investigate this a series of low-temperature neutron-scattering experiments were completed to probe the magnetic ground state. Measurements were done with long wavelength neutrons [2.3688(3) Å] for very long counting intervals at a medium flux source, but no evidence for long-range magnetic ordering was detected down to 4 K (see Fig. 6). Given the very small moment expected on the Re^{6+} spin-$\frac{1}{2}$ site, it is not clear that a complex ordering would be detectable using this technique. Thus, the diffraction patterns expected for a variety of simple ferromagnetic and antiferromagnetic arrangements were simulated using FULLPROF with a moment size of $1\mu_B$ on each site. Most fcc materials order in a few types of magnetic structures, and some of these were investigated in detail.[26,27] For example, a simple stacking of Re^{6+} moments of magnitude $1\mu_B$ in a type-I ordering $[Q=(0,0,1)]$ yielded Bragg peaks which were on the order of 2% of the intensity of the strongest structural peak. This is clearly within the detection limits of the instrument, and thus, if magnetic ordering of this type were present it would have been observed. While the evidence is to the contrary, the existence of magnetic ordering cannot be precluded on this basis alone. No significant lattice distortion, which may be expected with an ordering transition, was noted in the vicinity of T_G.

Magnetization measurements performed on this sample in fields up to 5.5 T provided further evidence for the absence of long-range magnetic order, since no saturation of the moment was found even to low temperatures (see Fig. 7). Evidence for hysteresis was observed, which was most prominent at 5 K, below T_G. As the temperature was increased, the size of the remnant magnetization was reduced greatly, until it was almost negligible at 40 K. Magnetic hysteresis is typical in spin-glass materials due to the large number of degenerate ground states that can be accessed at virtually negligible energy cost. By this criterion, then, and given the absence of any evidence for ferromagnetism, it is reasonable to conclude that Sr_2CaReO_6 is a spin glass. It is unusual, though, that spin-glass behavior would be observed at all,

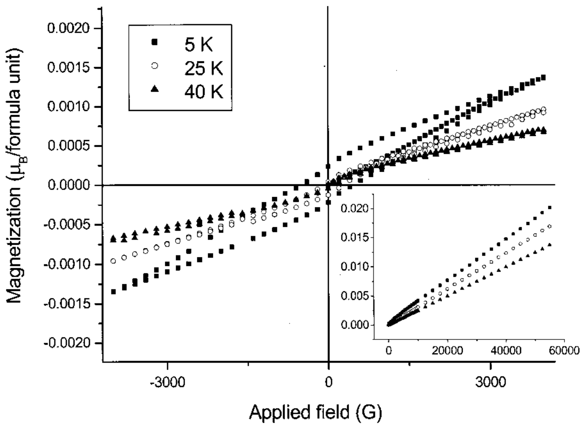

FIG. 7. dc magnetization measurements as a function of field for $T=5$ K, $T=25$ K, and $T=40$ K. Note the strong hysteresis at $T=5$ K. The inset shows the high field measurements, which show no signs of saturation.

since such systems arise due to chemical disorder on the magnetic sites, such as in the alloys CuMn.[28] The powder-neutron-diffraction results indicate no such disorder down to the 1% level of detectibility. There are cases of spin-glass behavior in the absence of disorder in other frustrated systems, such as $Y_2Mo_2O_7$ (which has $f_{\mathrm{frus}}\sim 10$), but in even this case, evidence for an ill-defined disorder has been claimed in recent x-ray absorption fine structure measurements.[29] Further measurements on Sr_2CaReO_6 may reveal small levels of disorder as well.

C. μSR measurements

μSR has long been used to study the dynamics of spin glasses and related systems. For small S-spin systems, in particular, muons are perhaps the best probe of the low-temperature magnetic ground state within a broad frequency range.

Figure 8 shows several zero-field-cooled scans taken between $T=2.5$ and 28 K. The two component nature of the spectra is immediately evident below $T_G\sim 14$ K, as opposed to the single-component high-temperature scans which is characteristic of a paramagnetic response. This characteristic two-component signal indicates a quasistatic distribution of internal magnetic fields developing below T_G, as noted in other spin glasses.[6,30] The fit to the spectra indicated in Fig. 8 are modeled after Uemura's original treatment of these line shapes in his pioneering μSR work on AuFe and CuMn alloys:[28]

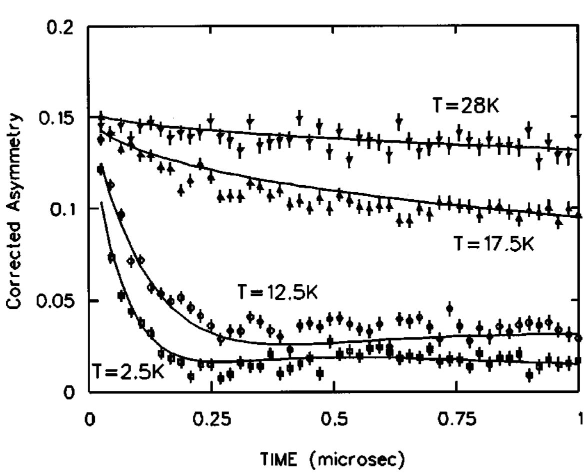

FIG. 8. ZF μSR measurements of Sr_2CaReO_6 at $T=2.5$, 12.5, 17.5, and 28 K. The fits are based upon a generic spin glass relaxation function as described in the text.

$$G(t)=\frac{1}{3}\{\exp[-(4\alpha_d^2 t/\nu)^{1/2}]\} + \frac{2}{3}\left[1-\frac{\alpha_s^2 t^2}{(4\alpha_d^2 t/\nu+\alpha_s^2 t^2)^{1/2}}\right] \times\exp[-(4\alpha_d^2 t/\nu+\alpha_s^2 t^2)^{1/2}]. \tag{4}$$

In this equation, ν is the spin fluctuation rate and α_s and α_d are the static and dynamic spin components. The fits to the spectra are more phenomenological than quantitative descriptions of the data. More detailed analysis which would include modeling of the spin-relaxation function for this system would be needed to extract a proper fluctuation rate, for example. It suffices to conclude at this point that the behavior is typical of a spin glass.

The relative absence of a fluctuating component in the spectra indicates that a large percentage of spins are frozen at low temperatures. Although the signal is weak due to the small moment, it is also clear that there is no periodic modulation in the line shape. This precludes the existence of magnetic ordering, which would show such a modulation due to muon precession in an ordered field.

Although this system is a typical spin glass from the μSR measurements, there are several departures from convention which merit further discussion. First, the signal is somewhat weak, which is expected due to the small magnetic moment, but since it is feeble, it is truly difficult to tell if there is a weak ordering signal buried in the background. There could indeed be short-ranged magnetically ordered clusters forming that are virtually undetectable by this technique. One would expect spin fluctuations at temperatures slightly higher than T_G to be visible in the spectra,[31] but the nature of the transition itself is rather abrupt, with only the slightest hint of a second component appearing at $T=17.5$ K. It is not surprising to see spin clusters starting to freeze out at temperatures higher than T_G, for our susceptibility measurements have a FC/ZFC divergence at $T\sim 23$ K. However, it is surprising that the second component develops quickly below T_G. The conventional way of understanding spin glasses is in the formation of islands of frozen spins which slowly develop as one passes through the transition. In our system, however, there is relatively little change in the muon signal from 12.5 to 2.5 K, which suggests that the spins freeze out rather abruptly. One can compare this behavior to what is seen in the related material Li_4MgReO_6, for example, which has a gradual formation of the glassy state as indicated by μSR measurements.[11] However, in this material, there is no cusp in the susceptibility, just a very weak FC/ZFC diver-

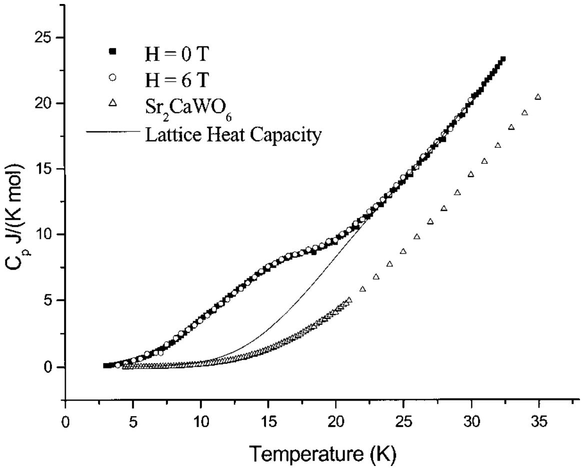

FIG. 9. The heat capacity of Sr_2CaReO_6 at $H=0$ T and $H=6$ T, the heat capacity of the lattice model compound Sr_2CaWO_6 at $H=0$ T, and the calculated lattice heat capacity of Sr_2CaReO_6 based upon the model material.

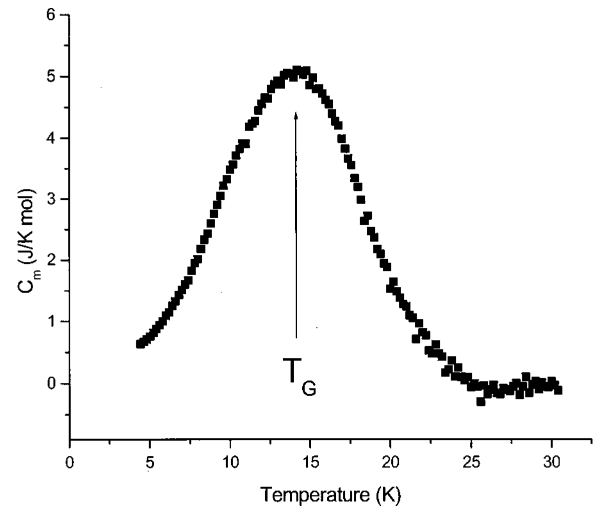

FIG. 10. The magnetic heat capacity of Sr_2CaReO_6 calculated by subtracting the lattice component.

gence at $\sim$12 K, and there is also the presence of disorder on the Mg/Li sites, but not the Re^{6+} sites.[11] In contrast, the pyrochlore $Y_2Mo_2O_7$ has no or very little disorder, but there are significant spin fluctuations observed with μSR and inelastic neutron scattering up to $\sim$40 K, and thus a very slow development of the spin-glass state as well.[6,31] The abrupt nature of the transition in Sr_2CaReO_6 is unusual and worthy of further investigation.

D. Heat capacity measurements

Although the μSR experiments provide compelling evidence for an unconventional spin-glass ground state, the existence of a long- or short-range magnetic ordering, for example, may be overlooked due to the local nature of the probe's interactions. For example, in the fcc antiferromagnet $GdInCu_4$,[26] a transition to a partially ordered state occurs in which glassy layers of Gd moments are interspersed with ordered layers. The magnetic susceptibility for this material is very similar to Sr_2CaReO_6, with a FC/ZFC divergence at temperatures higher than the cusplike feature, which is due to a weak ordering followed by a spin-glass transition. It is conceivable that μSR experiments would be relatively insensitive to this set of transitions, and other factors such as the existence of multiple oxygen sites for the muon to reside on may further complicate the interpretation of the results. Specific-heat measurements would provide more definitive evidence about the ground state. For example, a λ-like anomaly would be present in the case of long-range magnetic ordering, albeit diminished in magnitude due to the small moment. Spin-glass behavior, on the other hand, would result in a broad feature centered about T_G.

The results of the heat capacity measurements in an applied field of 0 and 6 T are shown in Fig. 9. A broad and smeared out anomaly is readily visible in the data in the vicinity of T_G, and there is no sign of a λ-type feature that would be expected for a magnetically ordered system. In addition, the robustness of the anomaly with respect to field is unexpected in conventional spin glasses.[32]

In an effort to extract the magnetic component to the specific heat, the nonmagnetic analog Sr_2CaWO_6 was synthesized and measured. Stoichiometric quantities of prefired $SrCO_3$, $CaCO_3$ (99.999%, Cerac), and WO_3 (99.98%, Alfa-Aesar) were intimately ground, pressed into pellets, and fired in air up to 1350°C for 12 h. A regrinding and refiring step was needed with rapid quenching to isolate the final product and avoid a Sr_2WO_5 impurity. The resulting product was orthorhombic, with lattice parameters in agreement with the literature[33] (see Table I). Unfortunately, the difference in the underlying lattice symmetry gave rise to a quantitatively different heat capacity, and a straight subtraction of the two data sets was not a feasible route to determining the magnetic heat capacity C_m. Instead, a different approach was taken. The Debye temperature as a function of temperature was determined for Sr_2CaWO_6 using the Debye specific-heat expression

$$C=9R(\theta_D/T)^3\int_0^{\theta_D/T}\frac{x^4e^x}{(e^x-1)^2}dx. \tag{5}$$

The same procedure was done for Sr_2CaReO_6, and the two data sets were scaled by a single constant such that the Debye temperatures were in agreement at temperatures higher than the magnetic transition. The lattice contribution for Sr_2CaReO_6 was then calculated down to low temperatures with the rescaled data, and subtracted from the total heat capacity to estimate the magnetic contribution (see Figs. 9 and 10). It is worth noting that the lattice contribution to the heat capacity is low compared to the magnetic contribution for the $T\sim T_G$ regime. This suggests that further calculations with the magnetic heat capacity, such as the entropy removal at low temperatures, will be relatively unaffected by details of the estimated lattice contribution.

The final result for C_m clearly accentuates the broad signature typical for short-ranged correlations that are seen in spin glasses (Fig. 10). The extensive nature of the peak suggests that magnetic correlations may set in at higher temperatures, which is echoed by the μSR measurements which in-

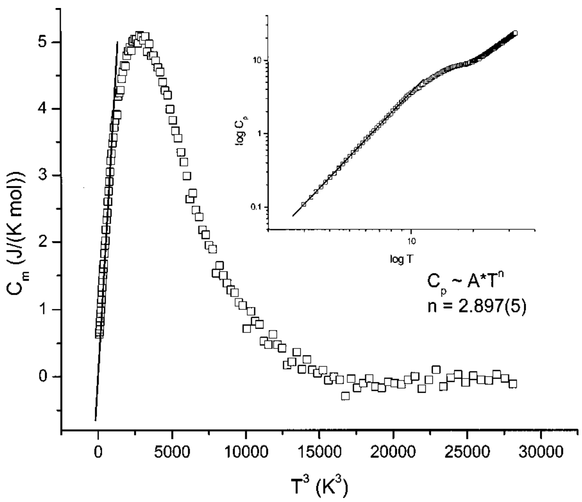

FIG. 11. The magnetic heat capacity of Sr_2CaReO_6 as a function of T^3. The inset shows the heat capacity as a function of temperature on a logarithmic scale (base 10), emphasizing the T^3 dependence.

dicate a slight glassiness as high as 17.5 K. It is interesting to compare the specific-heat anomaly with the susceptibility results, which show a broad peak as well centered about T_G, and a FC/ZFC dependence which diverges at higher temperatures (~23 K). This behavior is somewhat reminiscent of what is observed in the pyrochlore $Y_2Mo_2O_7$, which has a smeared out heat capacity anomaly that has been interpreted as a signal of short-ranged ordering at $T_G \sim 22.5$ K.[34] Subsequent neutron-scattering measurements have confirmed that these correlations persist to $T \sim 40$ K in the form of low-energy spin fluctuations. Further neutron work may show a similar result for the dynamics of Sr_2CaReO_6.

A striking difference between the two systems is the absence of a linear dependence of C_m with temperature for Sr_2CaReO_6 below T_G. This linear variation has been noted for $Y_2Mo_2O_7$ (Ref. 34) and related compounds such as $Y_2Mn_2O_7$ (Ref. 35) and suggests a low-temperature density of states which is independent of energy as would be expected for spin glasses. To determine the power law for Sr_2CaReO_6, a logarithmic plot of the heat capacity as a function of temperature was made (see Fig. 11, inset). The calculated exponent was 2.897(5) for $T < 10$ K. Since the lattice component should be negligible in this region, it is somewhat surprising to find $C \sim T^3$. The strong T^3 dependence is shown more clearly in Fig. 11, with an excellent fit to $C_m \sim T^3$. Unusual temperature dependencies of the heat capacity at low temperatures have been found in other frustrated systems, with the most notable example being SCGO, which has $C \sim T^2$ which has been ascribed to two-dimensional (2D) antiferromagnetic (AF) spin waves from large 2D correlated domains.[36] Another more recent example is the case of $LiNiO_2$, which has a complex spin-glass-like ground state and a $T^{2.5}$ specific-heat dependence.[37] One possible origin for the appearance of the T^3 term in Sr_2CaReO_6 is from spin waves. For a long-range ordered 3D AF, one would expect $C \sim T^3$ from a spin-wave contribution.[38] However, from the geometry of the frustrated lattice, and from the evidence presented previously in this paper, it is unlikely that this system exhibits long-range order, or at least it is unlikely that the bulk of the material orders. A more plausible explanation for this feature is that there is a difference in the dynamical response of this material when compared to other spin glasses rather than an ordering mechanism. In analogy with SCGO, which has large but finite 2D correlated regions of spins, one would expect Sr_2CaReO_6 to have large but finite 3D correlated regions of spins, and hence the T^3 heat capacity term in the absence of magnetic ordering.

It is possible that due to inhomogeneities in the sample, there may be regions of ordered clusters of moments, with the rest of the material remaining in a spin glass state. Theoretical studies on the nearest-neighbor fcc Heisenberg antiferromagnet have shown that spin dilution on the order of 15% is enough to drive the system from an ordered state to a spin-glass one.[39] It is possible that small levels of local disorder can generate separate domains of spin glassy and ordered states by this mechanism. Furthermore, these studies have shown that the transition to the long-ranged ordered state is very sharp and first order in nature. Evidence for an abrupt first-order transition is seen in the μSR experiments, but the heat capacity data do not show any sharp features. This feature may be obscured if there is only partial ordering in the sample, but even a sharp spike should be visible. It is indeed conceivable as well that the transition itself may be first order and spin glassy,[40] rather than due to regions of ordered and spin-glassy domains, but substantial proof to support either scenario is not available from this study. Indeed, the only evidence for the abrupt nature of the transition is in the μSR experiments, and this is only noted in the context of other spin glasses, which typically have very gradual transitions.

Integration of the low-temperature magnetic specific heat is a measure of the magnetic entropy by the following relationship:

$$S = \int_0^T (C_m/T)\,dT. \tag{6}$$

The total magnetic entropy integrated over the entire temperature range of the anomaly is 3.73 J/K/mol for 1 formula unit of Sr_2CaReO_6. This is ~64.7% of the expected value of $R\ln(2S+1)$ for 100% of the spins freezing. At the magnetic transition itself, only ~35.3% of the entropy is recovered, indicating that most of the entropy removal occurs above T_G, as would be expected for a spin glass.[32] One can compare these results with the monoclinic $S=1$ fcc ordered system Sr_2NiTeO_6 which shows a λ anomaly at $T_N \sim 28$ K indicative of magnetic ordering and a continuous phase transition.[14] Nonetheless, magnetic susceptibility measurements show evidence for magnetic correlations at $T \sim 35$ K by a FC/ZFC divergence at temperatures higher than the cusp at T_N. In this case, approximately 70% of the entropy is recovered at the magnetic transition, but the ground state is ordered rather than glassy. As the Ni^{2+} ions in Sr_2NiTeO_6 have $S=1$, this seems to suggest that it is the $S=\frac{1}{2}$ moment on Re^{6+} that induces the spin-glass ground state in Sr_2CaReO_6. Further experiments are clearly needed to explore this possibility.

CONCLUSIONS

Magnetic susceptibility, neutron scattering, μSR, and specific-heat data on the *B*-site ordered perovskite Sr_2CaReO_6 are all consistent with unconventional glass behavior below $T_G \sim 14$ K. Among the unconventional features are the thermal abruptness of the spin-freezing transition from μSR, the FC-ZFC divergence above T_G from susceptibility, and the very unusual T^3 dependence of the low-temperature specific heat. Further work is needed to explore the spin dynamics and magnetic microstructure of this material.

ACKNOWLEDGMENTS

The authors would like to thank Ron Donaberger for his technical assistance with the neutron-scattering experiments at Chalk River. The authors would also like to acknowledge M. J. P. Gingras for his critical reading of this manuscript. C. R. Wiebe gratefully acknowledges financial support for this work in the form of a PGS B from the National Sciences and Engineering Research Council, and a OGSST from the government of Ontario. This work was also supported through research grants to J. E. Greedan and G. M. Luke from the National Sciences and Engineering Research Council and to G. M. Luke from the Canadian Institute for Advanced Research. The MAGLAB experimental apparatus was purchased through funding from the CFI and ORDCF.

[1] G. Aeppli and P. Chandra, Science **275**, 177 (1997).
[2] A. P. Ramirez, in *Handbook of Magnetic Materials*, edited by K. H. J. Buschow (North-Holland, Amsterdam, 2001), Vol. 13, p. 423.
[3] J. E. Greedan, J. Mater. Chem. **11**, 37 (2001).
[4] O. Petrenko, C. Ritter, M. Yethiraj, and D. McK. Paul, Phys. Rev. Lett. **80**, 4570 (1998).
[5] S.-H. Lee, C. Broholm, G. Aeppli, T. G. Perring, B. Hessen, and A. Taylor, Phys. Rev. Lett. **76**, 4424 (1996).
[6] J. S. Gardner, B. D. Gaulin, S.-H. Lee, C. Broholm, N. P. Raju, and J. E. Greedan, Phys. Rev. Lett. **83**, 211 (1999).
[7] L. Pauling, *The Nature of the Chemical Bond*, 3rd ed. (Cornell University Press, Ithaca, 1960).
[8] M. J. Harris, S. T. Bramwell, D. F. McMorrow, T. Zeiske, and K. W. Godfrey, Phys. Rev. Lett. **79**, 2554 (1997).
[9] L. F. Feiner, A. M. Oles, and J. Zaanen, Phys. Rev. Lett. **78**, 2799 (1997).
[10] J. S. Gardner, S. R. Dunsiger, B. D. Gaulin, M. J. P. Gingras, J. E. Greedan, R. F. Kiefl, M. D. Lumsden, W. A. MacFarlane, N. P. Raju, J. E. Sonier, I. Swainson, and Z. Tun, Phys. Rev. Lett. **82**, 1012 (1999).
[11] M. Bieringer, N. P. Raju, G. Luke, and J. E. Greedan, Phys. Rev. B **62**, 6521 (2000).
[12] J. Longo and R. Ward, J. Am. Chem. Soc. **83**, 2816 (1961).
[13] R. Rodríguez, A. Fernández, A. Isalgué, J. Rodríguez, A. Labarta, J. Tejada, and X. Obradors, J. Phys. C **18**, L401 (1985).
[14] D. Iwanaga, Y. Inaguma, and M. Itoh, Mater. Res. Bull. **35**, 449 (2000).
[15] DICVOL version 24/11/98.
[16] B. L. Chamberland and G. Levasseur, Mater. Res. Bull. **14**, 401 (1979).
[17] D.-Y. Jung and G. Demazeau, J. Solid State Chem. **115**, 447 (1995).
[18] LSUDF: least square unit-cell refinement package run with GUCOS.
[19] A. W. Sleight, J. Longo, and R. Ward, Inorg. Chem. **1**, 245 (1962).
[20] FULLPROF version 3.5d, 1998.
[21] R. D. Shannon, Acta Crystallogr., Sect. A: Cryst. Phys., Diffr., Theor. Gen. Crystallogr. **A32**, 751 (1976).
[22] C. R. Wiebe, J. E. Greedan, G. M. Luke, J. S. Gardner, and I. Swainson (unpublished).
[23] A. Ferretti, D. B. Rogers, and J. B. Goodenough, J. Phys. Chem. Solids **26**, 2007 (1965).
[24] A. S. Wills, VALIST for Windows, 1998.
[25] R. Moessner and A. J. Berlinsky, Phys. Rev. Lett. **83**, 3293 (1999).
[26] H. Nakamura, N. Kim, M. Shiga, R. Kmiec, K. Tomala, E. Ressouche, J. P. Sanchez, and B. Malaman, J. Phys.: Condens. Matter **11**, 1095 (1999).
[27] J. S. Smart, *Effective Field Theories of Magnetism* (Saunders, Philadelphia, 1966).
[28] Y. J. Uemura, T. Yamazaki, D. R. Harshman, M. Senba, and E. J. Ansaldo, Phys. Rev. B **31**, 546 (1985).
[29] C. H. Booth, J. S. Gardner, G. H. Kwei, R. H. Heffner, F. Bridges, and M. A. Subramanian, Phys. Rev. B **62**, R755 (2000).
[30] G. A. Petrakovskii, K. S. Aleksandrov, L. N. Bezmaternikh, S. S. Aplesnin, B. Roessli, F. Semadeni, A. Amato, C. Baines, J. Bartolomé, and M. Evangelisti, Phys. Rev. B **63**, 184425 (2001).
[31] S. R. Dunsiger, R. F. Kiefl, K. H. Chow, B. D. Gaulin, M. J. P. Gingras, J. E. Greedan, A. Keren, K. Kojima, G. M. Luke, W. A. MacFarlane, N. P. Raju, J. E. Sonier, Y. J. Uemura, and W. D. Wu, Phys. Rev. B **54**, 9019 (1996).
[32] J. A. Mydosh, *Spin Glasses, An Experimental Introduction* (Taylor and Francis, London, 1993).
[33] F. Zhengmin, L. Wenxiu, and L. Dongcai, Sci. Sin. **26**, 835 (1983).
[34] N. P. Raju, E. Gmelin, and R. K. Kremer, Phys. Rev. B **46**, 5405 (1992).
[35] J. N. Reimers, J. E. Greedan, R. K. Kremer, E. Gmelin, and M. A. Subramanian, Phys. Rev. B **43**, 3387 (1991).
[36] A. P. Ramirez, G. P. Espinosa, and A. S. Cooper, Phys. Rev. Lett. **64**, 2070 (1990).
[37] Y. Kitaoka, T. Kobayashi, A. Koda, H. Wakabayashi, Y. Niino, H. Yamakage, S. Taguchi, K. Amaya, K. Yamaura, M. Takano, A. Hirano, and R. Kanno, J. Phys. Soc. Jpn. **67**, 3703 (1998).
[38] J. A. Eisele and F. Keffer, Phys. Rev. **96**, 929 (1954).
[39] C. Wengel, C. Henley, and A. Zippelius, Phys. Rev. B **53**, 6543 (1996).
[40] M. J. P. Gingras (private communication).